RIGA TECHNICAL UNIVERSITY
Faculty of Mechanical Engineering, Transport and Aeronautics
Institute of Mechanics and Mechanical Engineering

Mārtiņš Irbe
Doctoral Student of the Study Programme "Engineering Technology, Mechanics and Mechanical Engineering"

DYNAMICS ANALYSIS AND CONTROL OPTIMIZATION OF DEVICES FOR POWER GENERATION FROM FLUID FLOW

Summary of the Doctoral Thesis

Scientific supervisor:

Professor Dr. habil. sc. ing.
JĀNIS VĪBA

Professor Dr. habil. sc. ing.
IGORS TIPĀNS

RTU Press
Riga 2020

Irbe, M. Dynamics Analysis and Control Optimization of Devices for Power Generation From Fluid Flow. Summary of the Doctoral Thesis. Riga: RTU Press, 2020. 40 p.

Published in accordance with the decision of the Promotion Council "P-04" of 2 September 2020, Minutes No. 43.

The Doctoral Thesis was developed with the financial support of the Doctoral Research grant of RTU and Faculty of Mechanical Engineering, Transport and Aeronautics.

https://doi.org/10.7250/9789934225574
ISBN 978-9934-22-556-7 (print)
ISBN 978-9934-22-557-4 (pdf)

DOCTORAL THESIS PROPOSED TO RIGA TECHNICAL UNIVERSITY FOR THE PROMOTION TO THE SCIENTIFIC DEGREE OF DOCTOR OF SCIENCE

To be granted the scientific degree of Doctor of Science (Ph. D.), the present Doctoral Thesis has been submitted for the defence at the open meeting of RTU Promotion Council at 14.30 on 22 December 2020 at the Faculty of Mechanical Engineering, Transport and Aeronautics of Riga Technical University, 6B Kipsalas Street, Room 521.

OFFICIAL REVIEWERS

Professor Dr. habil. sc. ing. Grigory Panovko
Mechanical Engineering Research Institute of RAS, Moscow, Russia

Professor emeritus Dr. sc. ing. Ēriks Kronbergs
Institute of Mechanics, Latvia University of Life Sciences and Technologies, Latvia

Assistant Dr. sc. ing. Oļegs Jakovļevs
Institute of Mechanics and Mechanical Engineering, Riga Technical University, Latvia

DECLARATION OF ACADEMIC INTEGRITY

I hereby declare that the Doctoral Thesis submitted for the review to Riga Technical University for the promotion to the scientific degree of Doctor of Science (Ph. D.) is my own. I confirm that this Doctoral Thesis had not been submitted to any other university for the promotion to a scientific degree.

Mārtiņš Irbe ……. (signature)

Date: ……

The Doctoral Thesis has been written in Latvian. It consists of an Introduction; 3 chapters; Conclusion; 116 figures; 2 tables; the total number of pages is 105, including four appendix; the total number of pages is 150. The Bibliography contains 91 titles.

CONTENTS

GENERAL OVERVIEW OF THE THESIS

Topicality

The rigid body interaction with the fluid flow (here: air, water) in technology, technological processes, transport, everyday life, sports, and nature occurs at everyday use. One of the useful uses of these interactions is the possibility of obtaining energy from the interactions. This is possible if the fluid is moving against the object, the object is moving in the fluid, or both the fluid and the object are moving, e.g, a wind generator or a hydraulic turbine. The term ‘extract energy’ on a larger scale means additional activities related to energy savings in various processes, such as fuel economy, dependence on the shape of the car body, the finish time of the skeleton movement.

This completion of works covers the author’s and his colleagues’ research in three areas of interaction: a) skeleton interaction with ice and air; b) interactions between airflow and rigid body in the air; c) interaction between water flow and the rigid body in the water. The actuality of the topic is related to research in the field of “green energy”: to save or extract energy from the flow of fluid surrounding the globe.

Aim and Main Tasks of the Work

The aim of the work is to develop methods and methodologies to carry out fundamental research in the field of energy-saving in the motion of a rigid body along with the fluid or to extract energy from the fluid flow and to apply the theory of optimal synthesis. In addition, computer programs for process modelling have been developed and experimental studies in the wind tunnel and in nature have been performed, which confirm the validation of the theory.

The research carried out in the work in three main directions, as a thematically merged set of scientific publications, is as follows.

1. **Skeleton research.**
   - 1.1. The theory of optimal synthesis in the field of “green energy”: to save or extract energy from the flow of fluid surrounding the globe was adapted and tested.
   - 1.2. Skeleton experimental studies have been performed in Sigulda bobsled push-start facility.
   - 1.3. A mathematical interaction model of skeleton sled and ice (water layer) mechanical parameters of different ice conditions has been developed. Numerical tests of the model have been performed.
   - 1.4. A model of skeleton and ice-air local interactions has been developed, which has been tested numerically with computer modelling and experimentally in Sigulda bobsled push-start facility.
2. **Rigid body and air interaction research**
   - 2.1. Theory and methodology for the interaction of various forms of **moving** 2D rigid body objects with **fluid** have been developed.

2.2. Theory and methodology for the interaction of various forms of **stationary** 2D rigid body objects with the **fluid flow** have been developed.
2.3. Theory and methodology for the interaction of various forms of **moving** 2D rigid body objects with the **fluid flow** have been developed.
2.4. 2D computer modelling studies for parametric identification of interactions have been performed.
2.5. Parametric optimization of real models of obtaining different types of wind energy has been performed.
2.6. 3D experimental studies in a wind tunnel have been performed.
2.7. A new prototype of wind energy production rotor type has been developed, designed, and manufactured.
2.8. The results of the developed theory and practice of airflow interactions have been presented in a scientific book.

3. Investigations of rigid body and water interactions

3.1. The theory of fluid interaction for water flows has been applied and improved.
3.2. A theory has been developed for extracting the energy of a robotic variable area fishtail vibration in a fluid flow.
3.2. Theory and methodology for double plate vibration analysis in fluid flow has been developed.
3.3. 3D experimental studies in a wind tunnel for a double plate model have been performed.
3.4. Parametric optimization of the motor cover of the motorized SUP board fin has been performed.
3.5. A patent application has been developed for the generation of fluid flow-induced vibrations energy extraction with a linear generator.

Research Object

In this work, the main object of research is the interaction of a fluid (with an infinite number of degrees of freedom) model with a rigid body. Interaction here means the **forces of close interaction** between an infinite number of surface points on a solid body and an infinite number of fluid particles. During the reduction, the main vector of the force system and its main moment at any point, such as the centre of mass, must be determined. This allows the approximate differential equations of motion of a rigid body to further create and integrate numerically. If this is done, although roughly with accepted hypotheses, it is not necessary to use complicated “space-time” models, which are also approximate.

Research Hypothesis

The main hypothesis of the work is based on the basic hypotheses of Newtonian mechanics:

- superposition equation of motion for a fluid-particle system in differential form;
- the interaction of impact of fluid particles with a rigid body in the pressure zone;

- the pressure created by the fluid particles in the suction area;
- ignoring viscosity.

These hypotheses have been proven by computer experiments and tested in practice.

As a result, a new approximate scientific theory was developed. The new theory differs from the existing theories in that it is not necessary to perform experiments in fluid tunnels (to find empirical "Drag" and "Lifting" coefficients) before dynamic analysis of fluids and synthesis calculations.

Research Novelty

In studies of continuous fluid systems dynamics, it is difficult to describe the motion of an infinite degree of freedom (∞ DOF) system around a solid or deformable-body, respect to all other bodies, and the rules of the beginning of their flow. Therefore, in practice, approximate methods are used, such as RANS (Reynolds-averaged Navier–Stokes equations), a labyrinth of stationary bodies, to which a fluid of parallel velocity of particles begins to flow from a certain distance. At the beginning there is a transition process after which, taking into account the viscosity, a stationary flow occurs. This process can take up to a second or part of a second. It is not clear how to change the fluid mesh during flow when the body begins to move. Of course, it is possible to continuously change the geometric configuration of interaction after a few steps and ask the previous final rules. This requires a large amount of work.

The proposed method (theory) and methodologies suggest the use of classical mechanical methods for infinite particle flow and interaction with a rigid body surface, regardless of viscosity. As a result, it is possible to obtain dissipate forces by reduction of their principal vectors and principal moments at the centre of mass of the system. The obtained values allow us to form differential equations of body motion, which are numerically integrated accordingly. With the integration, it is possible to perform parametric optimization with a computer and synthesize new efficient systems for efficient use of energy during fluid movement or to create new "green energy" systems for fluid flow around a rigid body object.

Practical Application of the Thesis

The main results of practical use

1. The experimental results obtained on the Sigulda bobsled push-start facility and their approximation can be used in the modernization of existing structures and the design of new skeletons.
2. The developed mathematical model of the skeleton and various ice mechanical parameters (water layer) can be used to improve the results during the competition.
3. The developed model of skeleton and ice-air local interactions can be used in modelling the movement of other sports (luge, bobsleigh).
4. The developed theory and methodology for the interaction of 2D objects with fluid in three cases (stationary object, stationary fluid, both objects move) can be applied in the synthesis of new "green energy" objects, as well as in the design of flying machines.

5. The developed methodology and 2D computer modelling models for the analysis of interactions of prisms of different shapes (rhombus, triangle, star) can be applied in object shape optimization.
6. The developed methodology and manufactured equipment shall be used for testing new equipment in a wind tunnel.
7. A theory for the control of a robotic fishtail actuator can be used to restore energy in its stopping phase.
8. A new prototype of a rotor type for wind energy production has been developed, designed, and manufactured.
9. A patent application has been developed for the generation of fluid flow-induced vibrations energy with a linear generator.
10. The results of the developed theory and practice of airflow interactions have been presented in a scientific book.

List of Publications

Article in a collection of scientific publications or a chapter in a monograph indexed in SCOPUS or WOS database

1. Viba J., Beresnevich V., Irbe M. 2020. Synthesis and Optimization of Wind Energy Conversion Devices. *Design Optimization of Wind Energy Conversion Systems with Applications.* vol. I, ed. Maalawi Karam Y. (IntechOpen) p. 17.

Scientific articles indexed in SCOPUS or WOS database

2. Tipans I., Viba J., Irbe M., Vutukuru S. K. 2020. Investigation of dual varying area flapping actuator of a robotic fish with energy recovery. *Agron. Res.* 18, 1046–55.
3. Tipans I., Viba J., Irbe M., Vutukuru S. K. 2019. Analysis of non-stationary flow interaction with simple form objects. *Agron. Res.* 17, 1227–34.

Full-text conference papers published in conference proceedings indexed in SCOPUS or WOS database

4. Vutukuru S. K., Tipans I., Viba J., Irbe M. 2020. Form optimization and interaction analysis of plane symmetry prism in AIR. *Engineering for Rural Development.* vol. 19, pp. 739–46.
5. Spade K., Vaicis I., Vutukuru S. K., Irbe M. 2020. Analysis of granule layer impact interaction on vibrating 2D prism. *Engineering for Rural Development*. vol. 19, pp. 1463–9.
6. Irbe M., Cerpinska M., Gross K. A. 2019. *Investigation of vibration induced by sliding down an ice plane.* Vol. 800, KEM.
7. Irbe M., Gross K .A., Viba J., Cerpinska M. 2019 .Modelling of stiffness variability of skeleton sled on inclined ice plane. *Engineering for Rural Development.* vol. 18, pp. 1215–20.

8. Vutukuru S., Viba J., Tipans I., Viksne I., Irbe M. 2019. Analysis of flat plate vibrations by varying frontal area to the flow. *Engineering for Rural Development.* vol. 18, pp. 1408–14.
9. Gulbis J., Viba J., Irbe M., Spade K. 2019. Experimental optimization of annealing of cylindrical brass casings. *Engineering for Rural Development*. vol. 18, pp. 852–7.
10. Cerpinska M., Irbe M., Elmanis-Helmanis R. 2019. Swirling flow in Francis turbines depending on guide vanes opening position. *Engineering for Rural Development.* vol. 18, pp. 1435–40.
11. Tipans I., Viba J., Vutukuru S. K., Irbe M. 2019. Vibration analysis of perforated plate in non-stationary motion. *Vibroengineering Procedia.* vol. 25, pp. 48–53.
12. Irbe M., Gross K. A., Viba J., Cerpinska M. 2018. Analysis of acceleration and numerical modeling of skeleton sled motion. *Engineering for Rural Development.* vol 17, pp. 1401–6.
13. Cerpinska M., Irbe M., Elmanis-Helmanis R. 2018. Displacement of shaft during hydropower generator air gap measurements. *Engineering for Rural Development*. vol. 17, pp. 1673–8.
14. Cerpinska M., Irbe M., Elmanis-Helmanis R. 2018. Vibration of foundation for rotary screw compressors installed on skid mounting. *Engineering for Rural Development.* vol. 17, pp. 1997–2002.
15. Cerpinska M., Irbe M. 2017. Specifics of natural frequency measurements for floor vibration. *Engineering for Rural Development.* vol. 16, pp. 162–6.
16. Viba J., Beresnevich V., Irbe M., Dobelis J. 2017. The control of blades orientation to air flow in wind energetic device. *Energy Procedia.* vol. 128, pp. 302–8.
17. Viba J., Beresnevich V., Noskovs S., Irbe M. 2016. Investigations of rotating blade for energy extraction from fluid flow. *Vibroengineering Procedia.* vol. 8, pp. 312–5.
18. Viba J., Eiduks M., Irbe M. 2015. Double pendulum vibration motion in fluid flow. *Engineering for Rural Development.* vol. 14, pp. 434–9.

Publications in conference book of abstracts

19. Jansons, E., Irbe, M., Kalniņa, I., Gross, K. The Influence of Environmental Conditions on Sliding Over Ice: an Experimental Study from the Bobsled Push-Start Facility. In: *ECOTRIB 2019 7th European Conference on Tribology*, Austria, Vienna, 12-14 June 2019. Vienna: 2019, pp. 247–247.
20. Irbe, M., Jansons, E., Plūduma, L., Gross, K. The Effect of Runner Tension on Sliding over Ice at Different Ice Conditions. In: *ECOTRIB 2019 7th European Conference on Tribology*, Austria, Vienna, 12–14 June 2019. Vienna: 2019, pp. 180–180.

Three Scientific articles under review to be indexed in SCOPUS or WOS database

21. An article in journal "*Tribology international*" about the research reviewed in Chapter 1 of the promotion work (as a thematically unified set of scientific publications) entitled "Unveiling ice friction and air drag for faster sliding in winter sports".

22. An article in journal "*Latvian Journal of Physics and Technical Sciences*" about the research reviewed in Chapter 2 entitled "Optimization of energy extraction using definite geometry prisms in air".
23. An article in journal "*Latvian Journal of Physics and Technical Sciences*" about the research reviewed in Chapter 3 entitled "Resistance estimation for propulsion system of a motorized SUP board equipped with waterjet".

Two full-text conference paper under review to be published in conference proceedings indexed in SCOPUS or WOS database

24. *14th International Conference on Vibration Problems 2019* – conference paper on the research discussed in Chapter 1 of the promotion work entitled "Analysis of the skeleton sled with different runner stiffnesses sliding motion induced vibrations on an inclined ice track".
25. *43rd National Systems Conference on Innovative and Emerging Trends in Engineering Systems, 2019* – conference paper on the research discussed in Chapter 3 of the promotion work entitled "Varying Area Vibrating Structure in a Fluid for Energy Gain".

Inventions

26. LR patent No. 14978, 20.02.2015. Riga Technical University, "Method of controlling the operating mode of a single-mass vibrator on a flexible suspension", co-author.

Author's Contribution to Publications

All scientific publications have been written in collaboration with supervisors Professor Jānis Vība and Professor Igors Tipāns, as co-authors or consultants in the development of publications. The work on scientific publications was collectively planned and accomplished by the authors. The percentage of research work contributed by the author to scientific publications is summarized in Table 1.

Table 1

Contribution to the Development of Scientific Publications

Publication No.	Activity	Contribution
1.	Experimental equipment design, prototyping, wind tunnel experiments, object motion analysis and data processing	25 %
2.	Research of literature, simple form object analysis, numerical modelling and graphical representation	25 %
3.	Research of literature, design, prototyping, 2D flow simulation and motion analysis, wind tunnel experiments, data processing and graphical representation	35 %

Continuation of Table 1

4.	Rigid body shape geometry optimization analysis of fluid and body interactions	25 %
5.	Modelling of granular fraction motion using approximate force determination method for pressure and suction zones	15 %
6.	Research of literature, experiments in a climate simulation chamber, 3D sliding motion modelling, data processing, graphical representation and compilation	75 %
7.	Research of literature, experiments in Sigulda bobsled push-start facility, 2D sliding motion analysis for a model with 8DOF, data processing, graphical representation and compilation	75 %
8.	Analysis, optimization and synthesis of non-stationary fluid and body interaction, wind tunnel experiments, numerical modelling	25 %
9.	Parametric optimization	5 %
10.	Data processing	10 %
11.	Analysis, optimization and synthesis of non-stationary fluid and body interaction, wind tunnel experiments, numerical modelling	25 %
12.	Research of literature, experiments in Sigulda bobsled push-start facility, numerical modelling, data processing, graphical representation, validation and compilation	75 %
13.	Data processing	10 %
14.	Determination of natural frequencies with SolidWorks Simulation	10 %
15.	Vibration measurements	10 %
16.	Experimental equipment design, prototyping, wind tunnel experiments, data processing	30 %
17.	Experimental device design, prototyping, wind tunnel experiments, body motion analysis	25 %
18.	Development of experimental model, experiments in wind tunnel, data processing, graphical representation, numerical modelling	40 %
19.	Experiments in Sigulda bobsled push-start facility	10 %
20.	Research of literature, experiments in Sigulda bobsled push-start facility, numerical modelling, data processing, graphical representation, validation and compilation	80 %
21.	Research of literature, experiments in Sigulda bobsled push-start facility, numerical modelling, data processing, graphical representation, validation and compilation	60 %
22.	2D flow simulations, numerical modelling and graphical representation	25 %

Continuation of Table 1

23.	3D flow simulations, data processing and graphical representation	40 %
24.	Research of literature, experiments in Sigulda bobsled push-start facility, 3D model design, frequency analysis of skeleton construction, data processing, graphical representation, validation and compilation	80 %
25.	Research of literature, numerical modelling and graphical representation	25 %
26.	Development of experimental model	10 %

Structure of the Thesis and Main Results

The structure of the dissertation (as a thematically unified set of scientific publications) is summarized in 3 chapters.

In Chapter 1, skeleton research is performed and summarized in scientific publications No. 6, 7, 12, 14, 15, 19, 20, 21, and 24, with the three main topics covered:

1) the sliding motion of a body on ice surface (water layer) with various parameters of the mechanical properties of ice and aerodynamic drag;
2) development and testing of an analytical method for determining the coefficient of resistance of ice (water layer) and aerodynamic (air) coefficient using a skeleton sled in Sigulda bobsled push-start facility;
3) analysis of skeleton sled motion and structure vibrations.

The Chapter 2 summarizes the scientific publications of fluid (air) flow, No. 1, 3, 4, 5, 8, 11, 16, 17, and 22, with the four main topics covered:

1) analysis of simple rigid body shape in a non-stationary fluid flow;
2) vibration analysis of flat and perforated plate in a non-stationary fluid flow;
3) shape optimization and interaction analysis for a symmetrical prism in airflow;
4) optimization of energy production for prisms of a specific geometric shape from airflow.

The Chapter 3 summarizes other studies of fluid dynamics in scientific publications No. 2, 9, 10, 13, 18, 23, and 25 with the four main topics covered:

1) variable area rigid body structure vibrations in fluid flow for energy extraction;
2) The double drive of a variable area rigid body structure model for vibrations in a fluid flow for energy extraction and a mathematical model of the horizontal motion of one tail of a fish robot in a fluid;
3) vibration analysis of the double plate pendulum-type model in a fluid flow;
4) water resistance study of motorized SUP board drive fin shape.

Thesis for Assertion

1. Standard explanations found in the literature on interaction of fluid and rigid body are not accurate: it has been proved that the lowest pressure (lifting force) does not always occur at the visually longest fluid flow line (i.e., as the highest local velocity). In fact, there is a suction phenomenon, which then also reduces pressure.
2. Viscosity may be ignored in engineering calculations for fluid-solid interaction analysis. This is justified because all computer modelling programs (which respect viscosity) are also approximate.
3. In the analysis of air-rigid body interactions, the principle of superposition of non-stationary flows or relative motion can be applied, i.e., the interaction can be divided into two zones: the pressure zone and the suction zone. The laws of classical mechanics, including Brownian chaotic motion of particles, apply in both zones.
4. The approximate theory obtained in the description of the interaction between air and a rigid body can be applied to the engineering estimates for the description of interaction between water and solid. The viscosity increases and so does the density (up to ~1000 times).
5. The differential equations of fluid-rigid body interaction obtained in the work can be applied to solve analysis, optimization, and synthesis problems without using complex and time-consuming “space-time” programming approximate methods.

INTRODUCTION

The dissertation as a thematically unified set of scientific publications has been developed by participating in different practical study directions. The first part has been developed when participating in the ERAF practically oriented research "The quest for disclosing how surface characteristics affect slideability" by studying the vibrations. The second part has been developed thanks to the new theory of Professor Jānis Vība about the interaction of a rigid body object and an unstationary flow, where, by following the principles of classical mechanics, simplified analytic relations between liquid and a solid body in a flow where developed and tasks of analysis and optimisation were carried out. The third part of the work is an addition to the second part, with bigger stress on practical studies. To create a unified scientific publication set for the work's structural concept, the algorithm for the analysis, optimisation, and synthesis of dynamic equipment explained in the book by J. Vība[1] has been used. Based on this, the following work development stages were performed that are summarised in Table 2.

Table 2

Development Stages of the Dissertation as a Thematically Unified Set of Scientific Publications

Stages	Skeleton (air flow, water under the runners)	Fluid (air) flow	Other studies about fluid dynamics
Initial analysis of the problem	+	+	+
1. Optimization of main subsystems		+	
2. Analysis of the ideal law		+	
3. Synthesis of the structural scheme	+	+	+
4. Determination of parameters	+	+	+

Chapter 1. Skeleton research

1.1. Theory of optimal synthesis in the field of "green energy": to save or extract energy from the flow of fluid surrounding the globe, was adapted and tested.

1.2. Experimental studies of skeleton have been performed in Sigulda bobsled push-start facility.

1.3. A mathematical interaction model of skeleton sled and ice (water layer) mechanical parameters of different ice conditions has been developed. Numerical tests of the model have been performed.

[1] Я. Виба. "*Оптимизация и синтез виброударных машин.*" – Рига: Зинатне, 1988. 253 с.

1.4. A model of skeleton and ice-air local interactions has been developed, which has been tested numerically with computer modelling and experimentally in Sigulda bobsled push-start facility.

Chapter 2. Rigid body and air interaction research

2.1. Theory and methodology for the interaction of various forms of **moving** 2D rigid body objects with **fluid** have been developed.
2.2. Theory and methodology for the interaction of various forms of **stationary** 2D rigid body objects with **fluid flow** have been developed.
2.3. Theory and methodology for the interaction of various forms of **moving** 2D rigid body objects with **fluid flow** have been developed.
2.4. 2D computer modelling studies for parametric identification of interactions have been performed.
2.5. Parametric optimization of real models of obtaining different types of wind energy has been performed.
2.6. 3D experimental studies in a wind tunnel have been performed.
2.7. A new prototype of wind energy production rotor type has been developed, designed, and manufactured.
2.8. Results of the developed theory and practice of airflow interactions were presented in a scientific book.

Chapter 3. Investigations of rigid body and water interaction

3.1. The theory of fluid interaction for water flows has been applied and improved.
3.2. A theory has been developed for extracting the energy of a robotic variable area fishtail vibration in a fluid flow.
3.2. Theory and methodology for double plate vibration analysis in fluid flow has been developed.
3.3. 3D experimental studies in a wind tunnel for a double plate model have been performed.
3.4. Parametric optimization of the motor cover of the motorized SUP board fin has been performed.
3.5. A patent application has been developed for generation of fluid flow-induced vibrations energy extraction with a linear generator.

1. SKELETON (AIR FLOW, WATER UNDER THE RUNNERS)

This study is a part of fundamental study about the sliding ability of ice and processes between the runner and ice, where a specific model is being analyzed – skeleton-slider's movement on a steep ice plane. By using the solid physical state of water as an interlayer, it is possible to significantly reduce the impact of force of friction and increase the speed of motion, therefore making the sport more dynamic and exciting. To increase the applicability, an additional collaboration was developed with athletes and coaches (Latvian Olympic Skeleton team) who can give both practical advice and feedback about their observations on the track. Unlike other technical sports that use the skeleton and bobsleigh track (Fig. 1.1), only stiffness of the skeleton sled's runners can be regulated.

a) b)

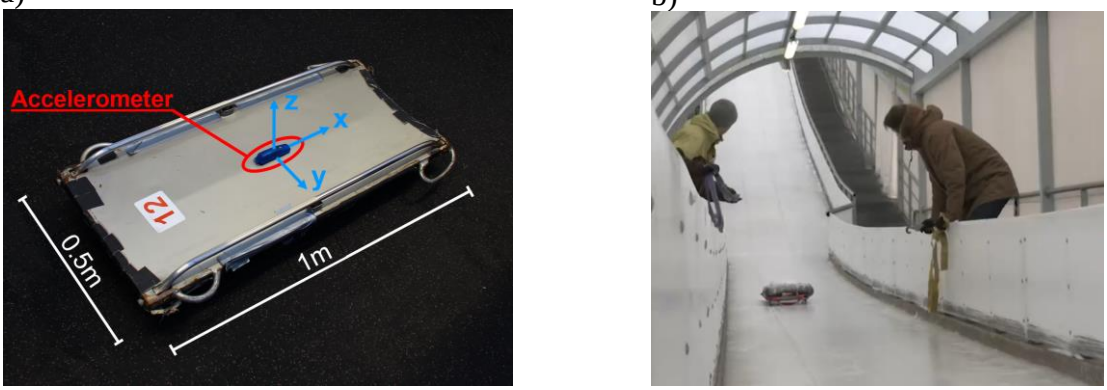

Fig. 1.1. a) skeleton with portable accelerometer and b) skeleton in motion down the ice track.

The construction of the sled is such that the runners work as tense springs between the rider and the surface of ice. It is a principal difference of the equipment used in other ice track sports. This means that, during the run, runners are exposed to complex pressure, meaning that there are significantly bigger local deformations, the runners are pressed and bent when entering and exiting the turns, and they are exposed to different vibrations when overcoming the uneven parts of ice, which are the issues of technical engineering research. The studies of the given dissertation can be divided into 3 stages.

1.1. Mathematical Model for a Skeleton With a Slider

In first stage a mathematical model is created to model the movement of skeleton-slider in an oblique plane, to analyse the contact surfaces (the unevenness of ice), and to discover the impact of runner's elasticity parameters on the sliding movement and how the result is affected by aerodynamic resistance coefficient (publications No. 6[2], 7[3], 10[4], and 12[5],

[2] https://www.scientific.net/KEM.800.298.
[3] http://www.tf.llu.lv/conference/proceedings2019/Papers/N424.pdf.
[4] http://www.tf.llu.lv/conference/proceedings2019/Papers/N229.pdf.
[5] http://www.tf.llu.lv/conference/proceedings2018/Papers/N179.pdf.

conference abstracts No. 19 and 20. A model of two degrees of freedom, Equation (1.1) describes the motion in *x*-axis direction:

$$m\ddot{x} = mg\sin\alpha - \mu\left(\begin{bmatrix}-c\left(z + A\sin x\right) - b\left(\dot{z} + A\dot{x}\cos x\right)\end{bmatrix} \cdot \left[\frac{1}{2} - \frac{1}{2}\operatorname{sgn}\left(z + A\sin x\right)\right]\right) - C_D\dot{x}^2. \tag{1.1}$$

The next equation describes the motion in *z*-axis direction (1.2):

$$m\ddot{z} = -mg\cos\alpha + \begin{pmatrix}-c\left(z + A\sin x\right)\\ -b\left(\dot{z} + A\dot{x}\cos x\right)\end{pmatrix} \cdot \left[\frac{1}{2} - \frac{1}{2}\operatorname{sgn}\left(z + A\sin x\right)\right], \tag{1.2}$$

where A is harmonic profile amplitude, m; g is acceleration do to the gravity, m/s^{-2}; μ is dry friction coefficient; c, b is stiffness and damping parameter from the runner and ice; $\dot{x}, \ddot{x}$ and $\dot{z}, \ddot{z}$ is velocity and acceleration, respectively; sgn is value +1 or –1 (ex., sgn = 1).

Skeleton sledge and slider centre of mass motion over a harmonic ice track surface profile is shown in Fig. 1.2.

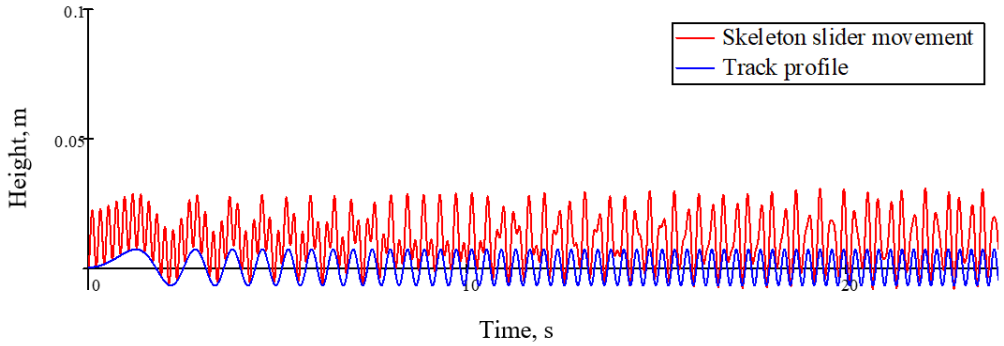

Fig. 1.2. Harmonic track profile and skeleton-slider centre of mass position in *x*-axis direction coinciding with time axis and *z*-direction shown as height.

1.2. Analytical Model for Determining the Air Drag and Sliding Friction

Second stage was carried out after the initial analysis of the problem during which two main skeleton-slider's sliding motion affecting parameters were identified – ice friction coefficient μ and aerodynamic resistance coefficient B_D. Hypothetical question is asked as to whether it is possible to determine both resistance force coefficients without using special laboratory equipment and circumstances, knowing only the time measurements and distances. And, using the direct integration method, find the velocity relation depending on the type of integration, time, and relocation. The aim of this subchapter is to create and test experimentally both methods of integration and determine numerically the precision of methods (publication No. 21 (under review, full paper in the appendix in promotion work)). Two methods are developed here to determine coefficients μ and B_D. One method takes into consideration the travelled time and the other method considers the distance travelled. These methods allow calculating resistance coefficients with input data from instantaneous velocity records with either time or distance records as presented in Fig. 1.3 a) and b), respectively.

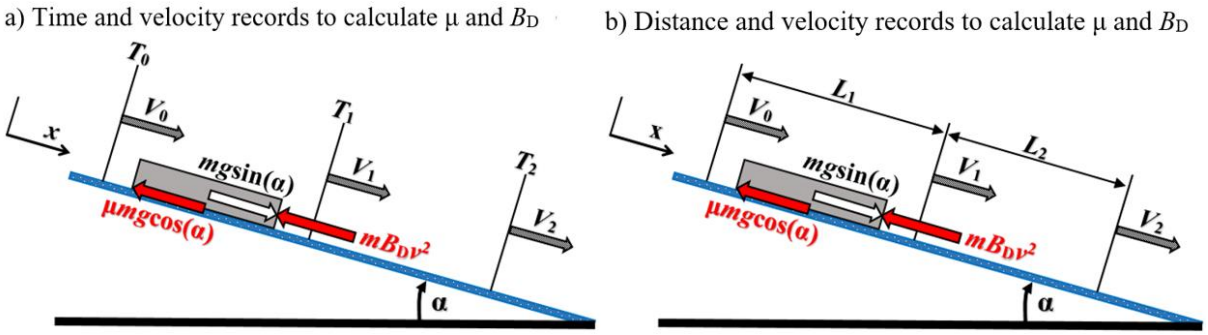

Fig. 1.3. Model showing the forces acting on the sliding body and the three sets of data: a) time and velocity; b) distance and velocity.

Equations of the first method for determining the coefficients (1.3) and (1.4):

$$\frac{a\tan\left(\frac{\sqrt{B_D}V_1}{\sqrt{\mu g\cos\alpha - g\sin\alpha}}\right)}{\sqrt{B_D\mu g\cos\alpha - B_D g\sin\alpha}} = -T_1 + \frac{a\tan\left(\frac{\sqrt{B_D}V_0}{\sqrt{\mu g\cos\alpha - g\sin\alpha}}\right)}{\sqrt{B_D\mu g\cos\alpha - B_D g\sin\alpha}}, \tag{1.3}$$

$$\frac{a\tan\left(\frac{\sqrt{B_D}V_2}{\sqrt{\mu g\cos\alpha - g\sin\alpha}}\right)}{\sqrt{B_D\mu g\cos\alpha - B_D g\sin\alpha}} = -T_2 + \frac{a\tan\left(\frac{\sqrt{B_D}V_1}{\sqrt{\mu g\cos\alpha - g\sin\alpha}}\right)}{\sqrt{B_D\mu g\cos\alpha - B_D g\sin\alpha}}. \tag{1.4}$$

Equations of the second method for determining the coefficients (1.5) and (1.6):

$$\frac{\ln\left[g\left(\sin\alpha - \mu\cos\alpha\right) - B_D v_1^2\right]}{2B_D} = -L_1 + \frac{\ln\left[g\left(\sin\alpha - \mu\cos\alpha\right) - B_D v_0^2\right]}{2B_D}, \tag{1.5}$$

$$\frac{\ln\left(g\left(\sin\alpha - \mu\cos\alpha\right) - B_D v_2^2\right)}{2B_D} = -L_2 + \frac{\ln\left(g\left(\sin\alpha - \mu\cos\alpha\right) - B_D v_1^2\right)}{2B_D}. \tag{1.6}$$

For comparison with other studies it was decided to calculate the average of the coefficient of friction from experiment runs giving a value of 0.0045. This value is ten times less than the value presented by Blau[6], but in a good agreement with the data presented by other investigators. Reading Fig. 5.8 (Blau, figure adapted from Tribology Handbook of 1991) shows that the friction coefficient for stainless steel and ice at –5 °C is about 0.03. Meanwhile, Poirier et al.[7] found the coefficient of friction to be around 0.0042. Makkonen *et al.*[8] used experimental data on ice friction with verification of a mathematical model over a wide range of ambient conditions. The comparison of this study with Makkonen *et al.* is illustrated in Fig. 1.4. In this work, the ice friction coefficient μ was 0.0043 for the third run in

[6] P. J. Blau (2008) Friction science and technology, From Concepts to Applications, Second Edition. CRC press. DOI: 10.1201/9781420054101.
[7] L. Poirier, E. P. Lozowski, S. Maw, D. J. Stefanyshyn, R. I. Thompson (2011) Experimental analysis of ice friction in the sport of bobsleigh Sport. Eng. 14 67–72. DOI: 10.1007/s12283-011-0077-02.
[8] L. Makkonen, M. Tikanmäki (2014) Modeling the friction of ice. Cold Reg Sci Technol, 102, pp. 84–93. DOI: 10.1016/j.coldregions.2014.03.002.

experiment at –5 °C. Analysis of slide movement by Makkonen *et al.* at an end velocity of around 8 m/s at –5 °C showed the ice friction coefficient μ to be around 0.0045.
The friction coefficient presented by Scherge *et al.*[9] was greater. The specific friction was obtained during experiments with a bobsled that was heavier than the skeleton in this study, explaining the greater friction. The difference can be viewed in Fig. 1.5, a modified figure from Scherge *et al.*

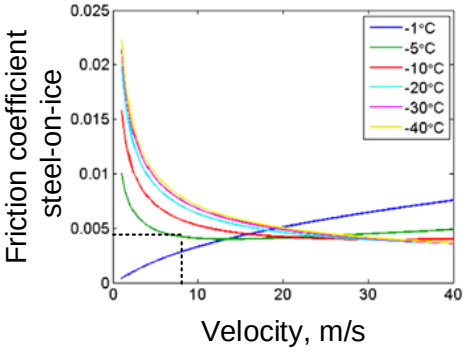

Fig. 1.4. Modelled friction coefficient μ steel-on-ice as a function of velocity at different temperatures, modified from Makkonen *et al.*

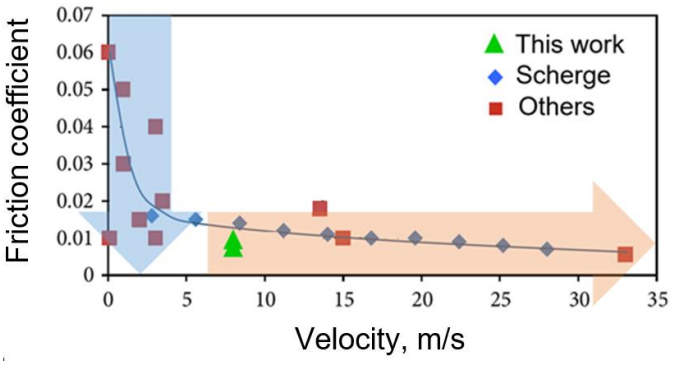

Fig. 1.5. Friction coefficient μ versus velocity with results of this work and of others, modified from Scherge *et al.*

1.3. Analysis of Skeleton Sled Sliding Motion Induced Vibrations With Different Runner Stiffness

In third stage, after mathematical analysis, the model is simulated with SolidWorkd Simulation. The task is to determine how the change of stiffness of skeleton's runners affects the natural frequencies of skeleton's sleigh construction structure. After processing the experimental data from ice track, the main dominant frequencies are gained, which are divided in those that define the motion's friction process and the ones that relate to structure's natural frequencies. The results are compared and analysed with a computer simulation in a 3D space (Fig. 1.6).

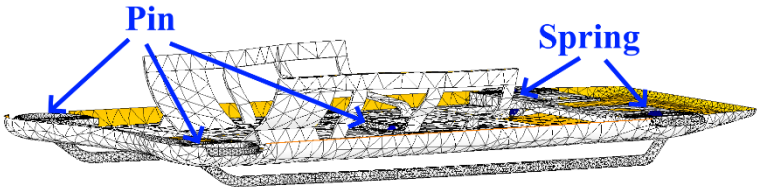

Fig. 1.6. 3D skeleton sledge model with simplified connections.

[9] M. Scherge, R. Böttcher, M. Richter, U. Gurgel (2013) High-speed friction experiments under lab conditions: on the influence of speed and normal force ISRN Tribol. 2013 1–7. DOI: 10.5402/2013/70320.

In addition, a simplified model to determine the natural frequencies in a 2D space for 6DOF chain system is created (Fig. 1.7), publication No. 24 (under publication process, full paper in the appendix of promotion work), additionally other construction vibration measurements are analysed, publications No. 14[10], 15[11].

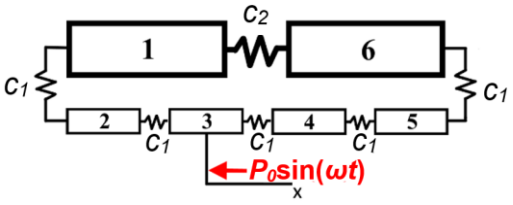

Fig. 1.7. The Skeleton and Slider Link Model.

From the analysis of experimental data records, the highest and most significant acceleration values are formed from the contact with the base. This is observed in the spectrum of vertical component a_z shown in Fig. 1.8. It has been experimentally determined how the runner's stiffness parameter r influences the dispersion of natural frequency measurements (Fig. 1.9). From the results obtained it can be concluded that the oscillations are on average with a frequency of about 71 Hz.

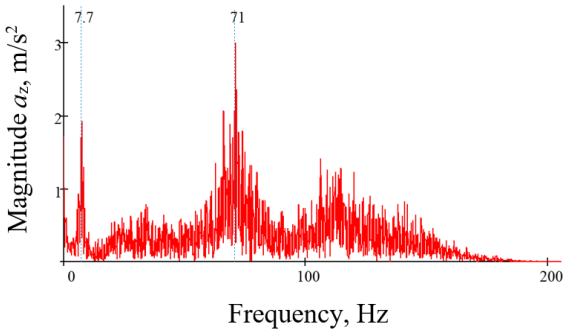

Fig. 1.8. Acceleration spectrum in *z*-axis direction.

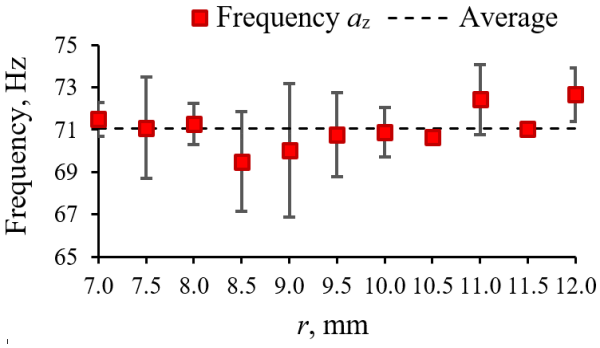

Fig. 1.9. Measured frequencies for skeleton sled structure vibrations in *z*-axis direction depending on runner stiffness radius *r*.

The results of 3D modeling show that increasing the spring tension increases the natural frequency. First twenty natural frequencies of the model were determined (Fig. 1.10). Similarly, 3D modeling results confirm that there is a good correlation between the natural frequencies' 15 Hz and 71 Hz locations in the entire range of the 20 modes (Fig. 1.10).

[10] http://tf.llu.lv/conference/proceedings2018/Papers/N094.pdf.
[11] http://www.tf.llu.lv/conference/proceedings2017/Papers/N031.pdf.

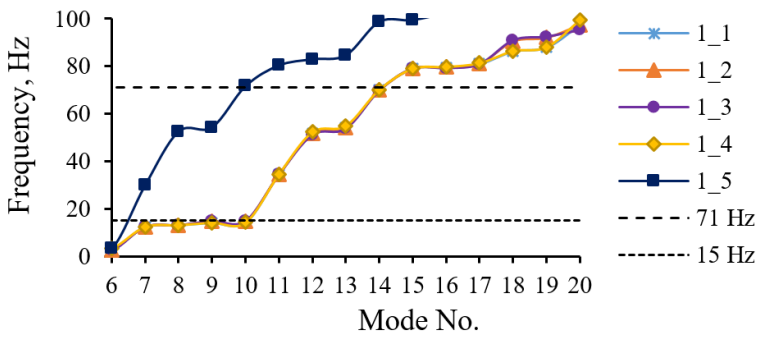

	c, $(N \cdot m^{-1})m^{-2}$	Load, N/m^2
1_1	Low	High
1_2	High	High
1_3	High	Low
1_4	Low	Low
1_5	Runer is fixed	

Fig. 1.10. Results from 3D skeleton sled frequency analysis with different spring stiffness and rigid connection (fixed runner).

The results of the analytical solution from the mathematical chain method model (Fig. 1.7) were obtained by solving equation (1.7)

$$\begin{aligned} &-4.100\,625\cdot 10^{71}\omega^{12} + 1.702\,706\,378\,269\,617\,706\,2\cdot 10^{78}\omega^{10} \\ &-2.330\,550\,006\,758\,863\,037\,2\cdot 10^{84}\omega^{8} + 1.173\,048\,438\,913\,584\,662\cdot 10^{95}\omega^{4} \\ &-1.655\,977\,938\,480\,901193\cdot 10^{95}\omega^{4} + 2.267\,791\,336\,595\,195\,112\,8\cdot 10^{99}\omega^{2} = 0, \end{aligned} \tag{1.7}$$

with the angular velocity ω argument function intersections with zero (Fig. 1.11).

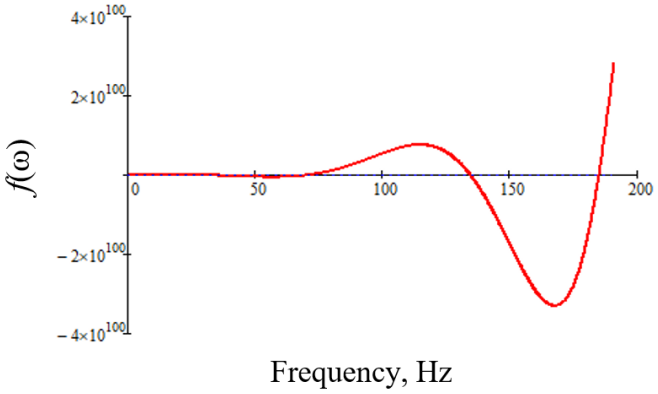

No.	Frequency, Hz
1	0
2	19.69
3	71.13
4	134.63
5	185.13
6	217.57

Fig. 1.11. Angular velocity function cross points with zero and resonance frequencies.

2. FLUID (AIR) FLOW

The second set of scientific publications of the dissertation is dedicated to the analysis of interaction of solid body in a fluid flow where a new analytical theory about interaction between air and water, if a solid body is moving in it or the other way around, is developed. Development and practical usage of this type of simplified method allows to analyse interaction of flow and different objects with much less resources needed without using difficult computer programs where calculations often are very time consuming. Given studies of the set of scientific publication can be divided in four subchapters.

2.1. Analysis of Non-Stationary Flow Interaction With Simple Form Objects

Simple form object analysis is given in Subchapter 1. An approximate method for determining forces that are related to interaction of fluid and a rigid body is offered. A mechanical system on a plane is looked at, which also is found in a fluid flow with an infinite amount of degrees of freedom (DOF), which is decreased to 5 DOF, 3 DOF for the rigid body and 2 DOF for pressure and vacuum/suction zones. Unstationary motion differential equations are made by the laws of classical mechanics. The approximate methods are numerically tested with the help of computer modelling. Fluid (air) interaction analysis is made for two types of geometrical rigid body objects – flat plate and a diamond-shaped object. The modelling results are used to specify the parameters of the offered approximate method. Theoretical results gained in the end of the section are used to analyse the movement of prismatic rigid body object to gain energy from the flow of liquid. Afterwards, flat plate parametrical optimization is made for the parameters of plate's motion velocity and rotation angle with the maximal power criteria (publications No. 1[12], 3[13], 5[14], 16[15], 17[16]).

The air flow interaction with the plate is subdivided in two phases: one interaction is on the pressure side and the other one – on the vacuum side (Fig. 2.1).

To analyze the air flow-plate interaction, the theorem on change of momentum of mechanical system in differential form is used, Meriam *et al.*[17] In accordance with this theorem the following equation can be written:

$$V\mathrm{d}m\cos\beta = \mathrm{d}N\mathrm{d}t, \tag{2.1}$$

where dm is an elemental mass of air flow; V is a velocity of air flow; β is the angle between air flow direction and normal to the plate surface L_1 (Fig. 2.1); dN is the impact force in the normal direction to the plate surface L_1; and t is time.

[12] https://www.intechopen.com/books/design-optimization-of-wind-energy-conversion-systems-with-applications/synthesis-and-optimization-of-wind-energy-conversion-devices.
[13] https://dspace.emu.ee/xmlui/handle/10492/4796.
[14] http://www.tf.llu.lv/conference/proceedings2020/Papers/TF365.pdf.
[15] https://www.sciencedirect.com/science/article/pii/S1876610217338377.
[16] https://www.jvejournals.com/article/17676.
[17] Meriam JL, Kraige LG and Bolton JN. Engineering Mechanics: Dynamics. 8th ed. New York: John Wiley& Sons; 2016. 736 p. ISBN: 9781119044819 1119044812.

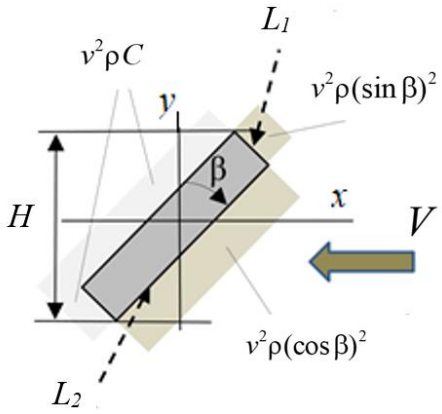

Fig. 2.1. Air flow interaction with rectangular flat plate.

Elemental mass dm of air flow can be mathematically described by equation

$$\mathrm{d}m = \rho VB\cos\beta \mathrm{d}t\mathrm{d}L, \tag{2.2}$$

where dL is elemental length of plate's surface; B is width of the plate (in the case of two-dimensional task B = const); ρ is the air density.

By integration of Equation (2.1) extra pressure and force along x-axis can be determined. Mathematically pressure distribution is described by the following expressions:

$$p_{L1} = V^2\rho\cos^2\beta, \tag{2.3}$$

$$p_{L2} = V^2\rho\sin^2\beta. \tag{2.4}$$

Vacuum side of the plate is loaded by constant pressure, which can be determined by formula

$$\Delta p_2 = V^2\rho C, \tag{2.5}$$

where C is constant to be found experimentally or by computer simulation.

This way, it is possible to find the total force applied to the body in the air flow. For example, projection on x-axis of total force F_1 applied to the rectangular plate is described by the following equation:

$$F_{xr} = -HBv^2\rho\left(C + \frac{\cos^3\beta + d\sin^3\beta}{\cos\beta + d\sin\beta}\right), \tag{2.6}$$

where d is the ratio of edges L_2/L_1; H is section height of the plate in the direction perpendicular to the flow.

As follows from the results obtained, an approximate analytical method can be applied to solve air flow and blade interaction problems. Validation of the results of analytical calculations can be performed using computer simulation and experiments. Examples will be discussed further. To determine coefficient C, numerical simulations in Solid Works for flat plate interaction with air flow were performed in publication No. 3.

2.2. Flat Plate Vibrations in the Fluid Flow

In this subchapter, the body's interaction is analysed, optimized and synthesized in order to analyse the vibrations that are created because of the interaction of fluid and a rigid body surface while changing the flat plate's angle regarding the flow. Here the main challenge is analysis, optimization, and synthesis of interaction between an unstationary fluid and a igid body. Space and time programming and approximate analytical methods are being used. An approximate analytical method is looked at where the interaction of object and the fluid flow is divided in two parts within the fluid interaction space. The first is the frontal side pressure part, which generates by using the law of change in amount of movement and which can be easily described in a differential form. In the second part, the interaction behind the plane is described, a side creating thin vacuum/suction. This thick vacuum/suction side is dependent also on the frontal zone flow interaction. The approximate analytical methods have been tested with experiments in a wind tunnel (publications No. 8[18], 11[19]).

A two-dimensional (2D) model of translation motion of thin flat plate (thickness $d \sim 0$) in co-ordinate plane xy is shown in Fig. 2.2. The model includes linear elastic element with stiffness coefficient c and linear viscous damper with damping coefficient b.

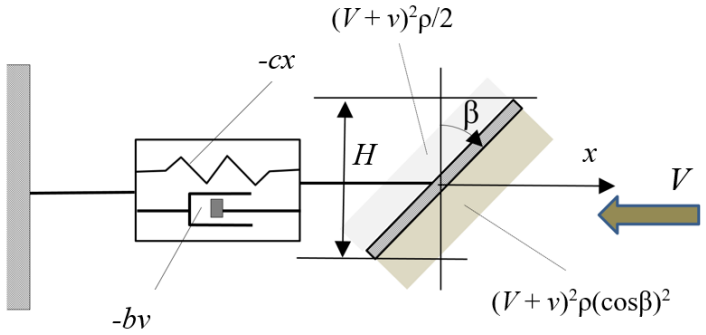

Fig. 2.2. Model of thin flat plate to obtain renewable energy from air flow.

In this case differential equation of plate motion along x-axis can be written in the following form:

$$m\ddot{x} = -cx - b\dot{x} - A\rho\left(0.5 + \cos^2\beta\right)(V+\dot{x})^2 \frac{V+\dot{x}}{|V+\dot{x}|}, \tag{2.7}$$

where $A = LB$ is a surface area of the plate; ρ is the air density; β is plate angle against air flow; m is mass of the plate; V is velocity of air flow; v is velocity of flat plate along x-axis; relative velocity $V_r = V + v$.

The renewable energy is generated due to the action of damping force ($-b\dot{x}$). Therefore, momentary power can be determined by formula

$$P = b\dot{x}^2. \tag{2.8}$$

[18] http://www.tf.llu.lv/conference/proceedings2019/Papers/N147.pdf.
[19] https://www.jvejournals.com/article/20801/abs.

The average power P_a during time t is determined by integration of Equation (2.8):

$$P_a = \frac{\int_0^t b\dot{x}^2 \mathrm{d}t}{t}. \tag{2.9}$$

By the analysis of Equation (2.7) it can be concluded that five parameters can be used to control the efficiency of this system. These parameters are as follows: *c*, *b*, *A*, β, and *V*.

Mathematical simulation of Equation (2.7) was performed with program MathCad. Results of simulation for control action by angle $\beta = (\pi / 2.5)\sin(7t)$ are presented in Fig. 2.3 and of simulation of plate's motion for the case of control action by velocity $V = V_0\left[2 - 0.5\sin(10t)\right]$ are presented in Fig 2.4.

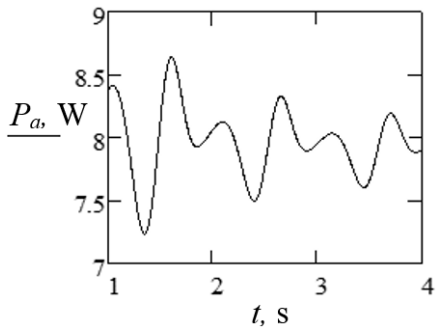

Fig. 2.3. Average power P_a of generator force $b\dot{x}$, case of control action on the system by harmonic variation of angle β.

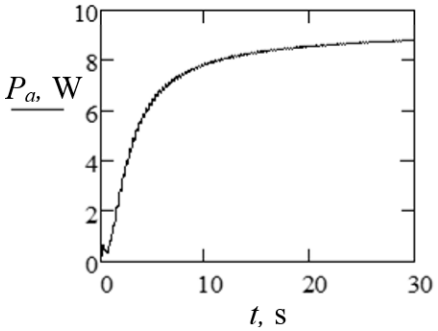

Fig. 2.4. Average power P_a of generator force $b\dot{x}$, case of control action on the system by harmonic variation of velocity *V*.

2.3. Form Optimization and Interaction Analysis of Plane Symmetry Prism in Air

In this subchapter, a form optimization has been done. The work is dedicated to the analyses of fluid (air) and solid body (prism) interactions to analyse optimization of form geometry while taking in account different criteria. To gain energy from the air flow, axially symmetric body is used, which has symmetrically aligned cuts circularly to change the size of cross-section area (Fig. 2.5).

A simplified mathematical model for technical engineering calculations is offered. For this model also the concepts of pressure and vacuum zone are used when exposing a body to fluid (air) flow. At the beginning all calculations are based on the assumption that the parameters of the body used in the research are unchanged. Afterwards, to improve the efficiency of the common system, the systemic parameters are changed using a constant step, while performing a detailed analysis of the reactions surface of the interaction between the fluid and the body. The mathematical equation has such assumptions: fluid (air) flow is laminar, incompressible (constant density), and fluid (air) viscosity is not taken into account (publication No. 4[20]).

[20] http://www.tf.llu.lv/conference/proceedings2020/Papers/TF170.pdf

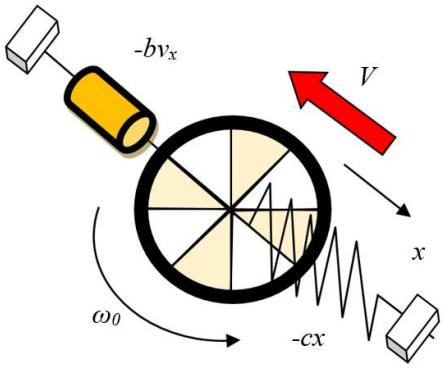

Fig. 2.5. Flat circular plate with alternate perforated quadrants: V – flow velocity; ($–bvx$) – generators force; ($–cx$) – spring force; ω_0 – angular velocity of rotating part.

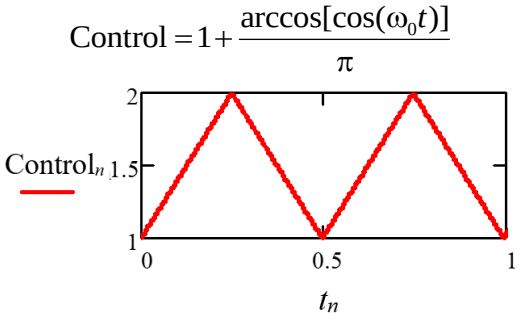

Fig. 2.6. Air flow interaction area as control action: C, A – constants.

Motion analysis in a 2D space is shown in Figs 2.7 and 2.8. Differential Equation (2.10) of plate motion with control is showed in Fig 2.6:

$$m\ddot{x} = -cx - \left(F_0 \operatorname{sgn}\dot{x} - b\dot{x}\right) + \left(1 + C\right) \cdot \frac{A}{\pi} \cdot \left\{\operatorname{acos}\left[\cos(\omega_0 t)\right] + \pi\right\} \rho(-V_0 - \dot{x})^2 \operatorname{sgn}(-V_0 - \dot{x}), \tag{2.10}$$

where m – mass; x – displacement; $\dot{x}$ – velocity; c – stiffness of linear spring, F_0; b – constants of linear generator damping; $(1 + C)$ – coefficient of pressing and suction sides interactions; V_0 – flow velocity; ω_0 – control actions harmonica angular frequency; A – constant area; ρ – air density; sgn – +1 or –1, depending of brackets signature.

The system considered consists of two concentric circular plates fixed at the centre, the plate the front area of which is subject to fluid flow is to rotate freely over the other circular plate (non-rotating), both plates have the same area and alternate perforated quadrants, the spring, and the linear generator in the incoming flow with a velocity V_0 (10 m/s).

The task of parametric optimization is as follows: to find a combination within the seven-parameter (m, c, F_0, b, ω_0, A, V_0) space with given constraints on the parameter values that provide the maximum power generated by the flow. It is to be noted that full resolution of such a task is not intended in this work. Note, however, that the best combination of the three parameters (m, c, ω_0) is close to the resonance zone: $\omega_0 = \sqrt{c/m}$. The graphs for this case are shown in Figs. 2.7 and 2.8.

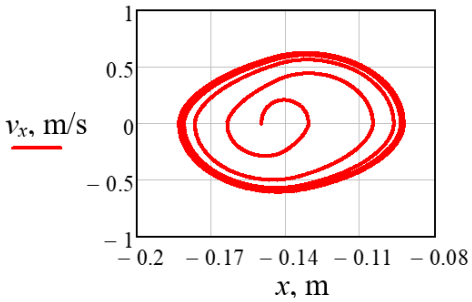

Fig. 2.7. Motion in phase plane: x – displacement; v – velocity.

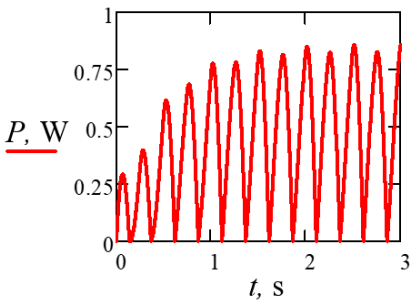

Fig. 2.8. Small plate power P: V_0 = 10 m/s; A = 0.2 m × 0.2 m; $\omega_0 = 4\pi$ s^{-1}.

2.4. Optimization of Energy Extraction Using Definite Geometry Prisms in Airflow

In thish subchapter, analytical method is described for analysing the interaction of moving or stationery bodies (prism) and for synthesizing motion in the air flow without using space-time programming numerical methods. To perform this, in engineering calculations a simplified fluid (air) particle and solid body interaction mathematical model has been used while using the law of change in the amount of motion. Interaction of the solid body (prism) and air has been looked at in different cases: a moving body (prism) in the air; still body (prism) in the airflow; moving body (prism) in the airflow. The difficult task of interaction between the solid body and air has been simplified by using the principles of superpositioning, i.e., taking into account the flows upwards and downwards (or backwards and in front) of the areas of the rigid body. It is determined how in these two areas the zones of pressure and suction are created with analytically calculable air pressures that are dependent from the flow velocity square and the body's shape. All equations are created based on the laws of classical mechanics. When creating the approximate mathematical model, forces of viscosity are not taken into account. Numerical results of interaction between different prisms and air flow are being compared, and the theoretical results of those are looked in detail. The mathematical model in this work is only applicable for those bodies, which have undergone a straight broadcast motion (publication No. 22 (in publication process, full paper in the appendix on the promotion work)). Mathematical model is described in the case of definite geometry shaped prism (Fig. 2.9).

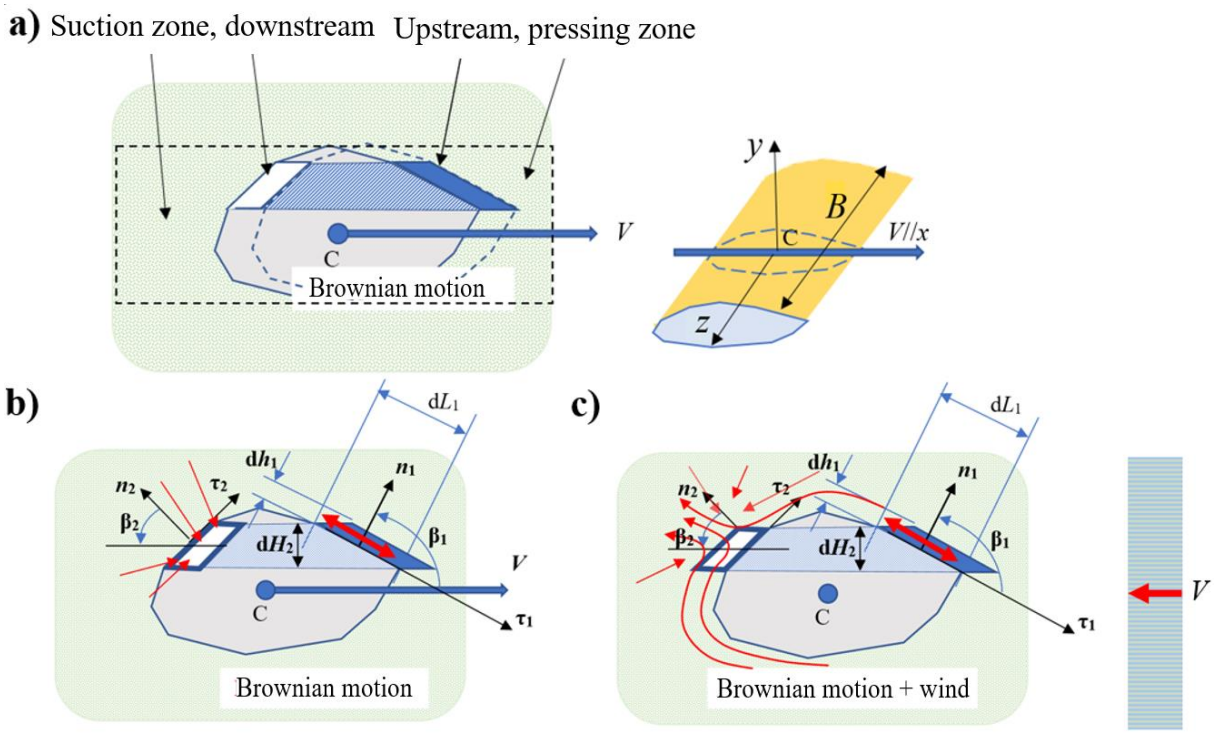

Fig. 2.9. Prismatic model: a) external relative flow over moving-prism in a very low speed airflow; b) interaction of the rectilinear translation (non-rotating) motion body in windless air; c) model of air interactions with stationary prism.

Considering the very small air element in the pressure zone, we use the momentum change in the differential form. According to the principle proposed in the present work (superposition principle), taking in the projection of the area normal n_1, before and after collisions (fluid-body interaction), we obtain Equation (2.11), from Brownian interaction to prism:

$$\begin{aligned} &m_{10}V_{B1} - (-m_{10}V_{B1}) = -N_1 \mathrm{d}t, \\ &m_{10} = V_{B1} B \rho \mathrm{d}t \mathrm{d}L_1, \\ &p_{10} = \frac{|N_1|}{B \mathrm{d}L_1}, \end{aligned} \tag{2.11}$$

where m_{10} is Brownian interaction mass; V_{B1} is an average air normal velocity in pressure zone; N_1 is normal force to small element from air; dt is infinitive small time interval; dL_1 is width of small element; B is prism height, perpendicular to the plane of motion; ρ is density of air; p_{10} is atmospheric pressure in pressure zone.

From prism air interaction at wind-ward side (pressure side)

$$\begin{aligned} &m_1 v \cos\beta_1 - 0 = -\Delta N_1 \mathrm{d}t, \\ &m_1 = v B \rho \cos\beta_1 \mathrm{d}t \mathrm{d}L_1, \\ &\Delta p_1 = \frac{|\Delta N_1|}{B \mathrm{d}L_1}, \end{aligned} \tag{2.12}$$

where m_1 is prism and air interactions boundary layer mass; v is prism velocity; β_1 is angle between velocity v and normal n_1; ΔN_1 is additional normal force, acting to prism; Δp_1 is pressure increase in pressing zone.

From the system of six Equations (2.11), (2.12) it is possible to find six unknowns. The two unknowns are required to solve the following calculations:

$$p_{10} = 2V_{B1}^2 \rho dt, \tag{2.13}$$

$$\Delta p_1 = \rho v^2 \mathrm{d}t \cos^2 \beta_1. \tag{2.14}$$

Accordingly, it is possible to apply Equations (2.11)–(2.14) in the suction zone (leeward side). However, the task is a little complicated with the amount of momentum differentials in the suction zone: it is not clear how to simplify the equations in differential form. Therefore, it is suggested to use one or the other hypothesis. Hypothesis should be tested experimentally or by using computer applications programs.

The first hypothesis. In suction zone pressure reduction Δp_{21} over the entire surface is constant and proportional to the square of the velocity v. We get

$$\Delta p_{21} = -\rho C_1 v^2, \tag{2.15}$$

$$p_{20} = 2V_{B2}^2 \rho dt, \tag{2.16}$$

where C_1 is a constant found according to experimental or numerical modelling; V_{B2} is average air normal velocity in suction zone.

The second hypothesis. In suction zone pressure reduction Δp_{22}, over the entire surface is not constant, but is proportional to the square of the velocity v, and also depends on normal n_2 to the surface area and also position angle β_2, thereby we obtain

$$\Delta p_{22} = -\rho C_2 v^2 \cos\beta_2, \tag{2.17}$$

$$p_{20} = 2V_B^2 \rho dt, \tag{2.18}$$

where C_2 is a second constant found in the same way as C_1.

The obtained differential relationships (2.13)–(2.18) can be used in engineering analysis and synthesis tasks in the low speed range. To do this, the prism parameters of the given configuration must be used along with the solution for the integral equations for the object surface.

For practical engineering calculations, it is recommended to adopt $V_{B1} = V_{B2}$ for low velocity $v << V_{B1}$ and $v << V_{B2}$ ranges. Then $p_{01} = p_{02} = p_0$, where p_0 is the mean atmospheric pressure around a given prism.

2.4.1. Optimization of Triangle Prism in Rectilinear Translation Motion in Airflow

The motion model with given length and angles is shown in Fig 2.10, where $R^{(e)}$ and $M_z^{(e)}$ are the external forces and moment providing rectilinear translation motion of triangle prism.

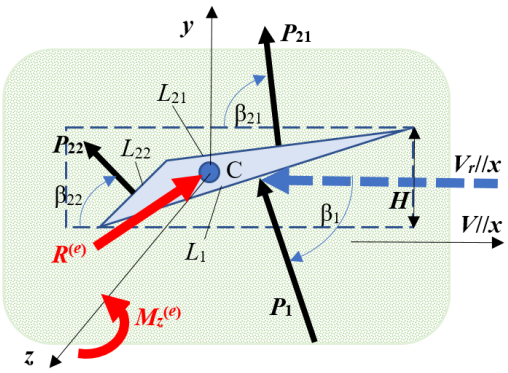

Fig. 2.10. Triangle prism movement in the wind direction V_r // V // x.

The optimization task should determine the prism braking velocity V that provides the maximum power in the mechatronic system. The differential equation of motion will be as follows:

$$m\ddot{x} = -(V_0 - V)^2 C_0 + Q. \tag{2.19}$$

Here, $C_0 = B\rho\left[\left(L_1\cos^3\beta_1 + C_2\cos\beta_{21}\right)^2 L_{21} + C_2\cos^2\beta_{22}\right]L_{22}$, where m is a prism mass; $\ddot{x}$ is constrained acceleration along x-axis; Q is braking force.

The task of optimization is as follows. Given for motion parameters C_0, m is for stationary motion when acceleration is zero ($\ddot{x} = 0$). Force Q of the prismatic braking mechatronic system shall be found to provide the maximum power P produced by the airflow force.

In the given case, without limitation, there is one optimal solution as given by (2.20):

$$V = \frac{V_0}{3}, \quad P = \frac{4C_0V_0^3}{27}, \quad Q = \frac{4C_0V_0^3}{9}. \tag{2.20}$$

As can be inferred from Equation (2.20), (if the flow rate V_0 changes) the real system requires a mechatronic force control Q system.

2.4.2. Motion of a Sharpened Prism in a Vertical Plane

We observe the movement of a sharp prism in a vertical plane when angles are equal $\beta_{22} = \beta_{21} = \beta_1$ (Fig. 2.11).

According to the first model theory mentioned above (use of constant C_1), the motion of a sharpened prism in a vertical plane is described by differential Equations:

$$m\ddot{x} = -[\rho LB(\dot{x}\sin\alpha - \dot{y}\cos\alpha)^2(1+C_1)\sin\alpha \cdot \mathrm{sgn}(\dot{x}\sin\alpha - \dot{y}\cos\alpha)\sin\alpha], \tag{2.21}$$

$$m\ddot{y} = \left[\rho LB\left(\dot{x}\sin\alpha - \dot{y}\cos\alpha\right)^2\left(1+C_1\right)\sin\alpha \cdot \mathrm{sgn}(\dot{x}\sin\alpha - \dot{y}\cos\alpha)\cos\alpha\right] - mg, \tag{2.22}$$

where, $\ddot{x}$ and $\ddot{y}$ are acceleration projections; α is angle between normal and vertical direction; sgn is a ±1 depending of function in brackets; g is free fall acceleration.

The obtained equations allow solving analytical and parametric optimization problems for a given non-stationary motion case. In addition, it should be noted that this movement is close to the bird's gliding or diving movement in the air.

Example of a diving motion calculation is shown in Figs. 2.11–2.14. All parameters are in system SI: $\rho = 1.25$; $LB = 0.04$; $mg = 2$; $C_1 = 0.5$; $\alpha = \pi / 4$.

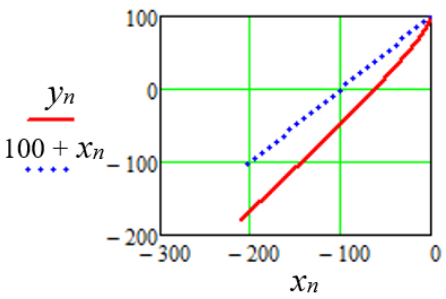

Fig. 2.11. The trajectory of the centre of mass motion in the vertical plane, starting from coordinates (x, y) = (0, +100).

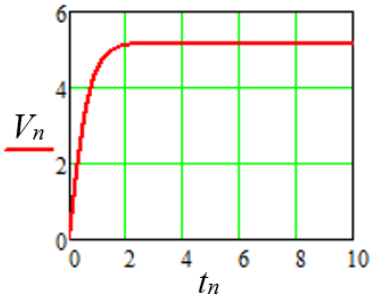

Fig. 2.12. Speed projection on prism, normal.

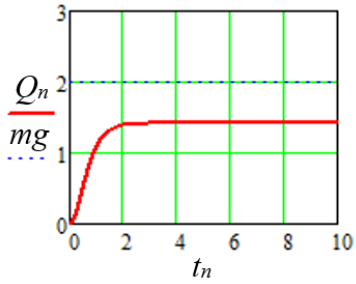

Fig. 2.13. Frontal force of air interaction.

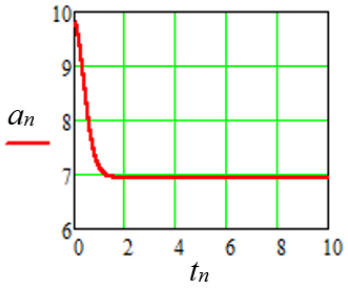

Fig. 2.14. Total acceleration of prism's fall and lateral slip. The figure shows that the viscous forces mentioned in the beginning of the article are not taken into account.

The obtained modelling results show that the velocity projection perpendicular to the sharp prism reaches the terminal value and does not change further. However, there is no acceleration component in this direction. Accordingly, the acceleration in the tangent direction becomes constant, but the velocity component increases linearly with time. This means that in real-world applications, viscosity must be observed or a real prism with a blunt front surface must be considered.

3. OTHER STUDIES OF FLUID DYNAMICS

The demand for autonomous efficient on-board energy devices is very high today, especially when doing tasks with an unmanned equipment where energy recovery from the environment is critical. Autonomous vehicles powered by liquids have the possibility of using different energy production methods in combination with a traction drive mechanism. Here, in the first two subsections of Part 3 of the dissertation, the drive of the fish tail principle with plane bending/vibration to ensure movement is considered. A flexible area-changing type vibrating (tail or wing) structure is better to increase energy efficiency compared to fixed area type designs, but the main disadvantage of such a flexible structure is that it is affected by the viscous nature of the given fluid. This study focuses on the development of a new approach to energy extraction for recharging an on-board battery from the environment. The goal is to create an autonomous vehicle using structural vibrations with a variable area (perforated plate like a tail fin). Robotic fish are designed so that the fins of the tail use water while moving, but draw the tail out of the water in the air flow during charging. The amount of battery space required is reduced, reducing weight and space. This results in negative aspects as well, many energy recovery steps must be performed in order to charge, consuming more time to complete the task. All the equations characterizing the process are developed in accordance with the classical laws of mechanics (more information about the study is available in publications No. 2[21] and 25 (under publishing process)). In addition , it is necessary to note the work on the research of the Francis turbine-type power plant, flow-induced vibrations and their effects in different operating modes, which is described in more detail in publication No. 13[22].

3.1. Mathematical Model of the One-Tail Robot Horizontal Motion in Fluid

We consider the motion of a simplified, one-tail actuator for horizontally diving robot (Fig. 3.1). Assuming a simple linear motion for the robotic fish in water with a mechatronic system, it is possible to come up with a triangular tail with flapping/curvilinear oscillations around axis O for a given time function. The hull and the tail are described as a mechanical system of one degree of freedom (1 DOF) defined by coordinate *x*. In order to avoid additional movement from the tail rotation leading to instability, it is considered that the rotation axis *O* coincides with the centre of mass of the tail fin for the robotic fish. Thereby, the differential equation for the robot motion will be

$$\left(m_0 + m\right)\ddot{x} = -N_{1x} - N_{2x} - b\dot{x}^2\,\mathrm{sgn}(\dot{x}), \tag{3.1}$$

where m_0 is a mass of the hull; m is a mass of the tail; $\ddot{x}, \dot{x}$ are correspondingly the acceleration and velocity of the hull; N_{1x} is a fluid interaction component in a pressing zone; N_{2x} is a fluid interaction component with the tail in suction zone; $b\dot{x}^2$ is non-linear interaction of the hull with fluid in rectilinear motion, depending of motion velocity $v = \dot{x}$; b is constant.

[21] https://agronomy.emu.ee/wp-content/uploads/2020/06/AR2020_Vol18SI1_Tipans.pdf.
[22] http://www.tf.llu.lv/conference/proceedings2018/Papers/N092.pdf.

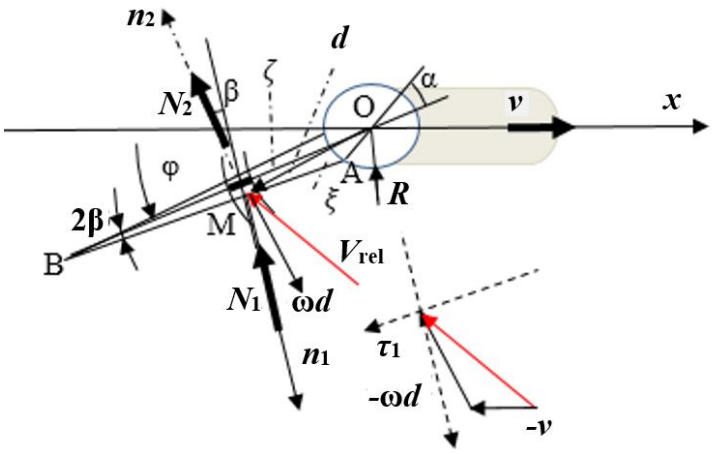

Fig. 3.1. The tail-fluid interaction calculation model.

To determine the vector components *N*1*x* and *N*2*x*, the interactions on two infinitely small tail areas in the pressure and suction zones are considered, as shown in Fig 3.1. The direction of the angular velocity of the tail rotation as well as the direction of relative motion of the housing must also be taken into account. Since the rotational velocity component of a given area depends on the distances to the axis of rotation, that is expressed by Equation (3.1) as an integral-differential equation, which can be solved approximately by using numerical methods.

Before integration, we write analytical link Equations (3.2) and (3.3) at pressing (upstream zone) for triangles OAB and OMB Fig. 3.1:

$$\xi = \frac{R\sin\gamma}{\sin\left(\alpha+\beta-\gamma\right)}; \tag{3.2}$$

$$d = \frac{R\sin(\alpha+\beta)}{\sin(\alpha+\beta-\gamma)}, \tag{3.3}$$

were ξ, d and R are shown in Fig. 3.1, but angle γ is $\measuredangle$ MOB.

According to engineering calculation method described in previous chapter to determine forces N_{1x} and N_{2x}, we first find forces in normal direction N_1, N_2 (Fig. 3.1). They depend on relative velocity projection squares as given by (3.4), (3.5):

$$\left|N_1\right| = B\rho\left|\int_0^{\beta}\left(v\sin(\varphi-\beta)+\omega\xi\right)^2 \mathrm{d}\xi\right|; \tag{3.4}$$

$$\left|N_2\right| = B\rho C\left|\int_R^{R_2}\left(v\sin\varphi+\omega\zeta\right)^2 \mathrm{d}\zeta\right|, \tag{3.5}$$

where ξ is a distance from side AMB and $\mathrm{d}\xi$ is a differential of ξ, both calculated by (3.3); ζ is a radial distance along OB; C is a constant, approximately equal to 0.5 (described in previous chapter).

For the approximate solution of Equation (3.1), force N_{1x} and N_{2x} can be taken for (3.6) and (3.7):

$$F_{1x} = |N_1| \cdot \operatorname{sgn}\left[v\sin(\varphi - \beta) + \omega \frac{R + R_2}{2} \right] \sin(\varphi - \beta); \tag{3.6}$$

$$F_{2x} = |N_2| \cdot \operatorname{sgn}\left(v\sin\varphi + \omega \frac{R + R_2}{2} \right) \sin\varphi. \tag{3.7}$$

An example of numerical modelling is given further with parameters R = 0.05 m; R_2 = 0.25 m. For the tail fin rotation angle and angular velocity is given by (3.8) and (3.9):

$$\varphi = a\left[\sin(pt) + 2\lambda_3 \sin(3pt + \varepsilon_3)\right]; \tag{3.8}$$

$$\omega = a\left[\sin(pt) + 6p\lambda_3 \cos(3pt + \varepsilon_3)\right], \tag{3.9}$$

where $\varepsilon_3 = -1.571$; $\lambda_3 = \pm 0.1$; $p = 5$ and $a = 0.5$.

Numerical modelling results in Figs 3.2–3.7.

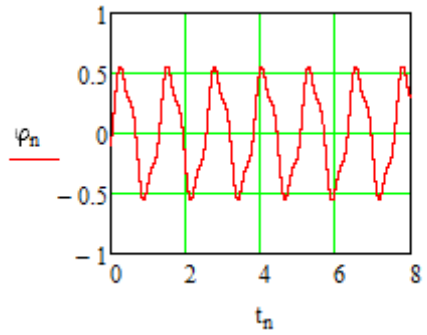

Fig. 3.2. Tail rotation angle for varying time.

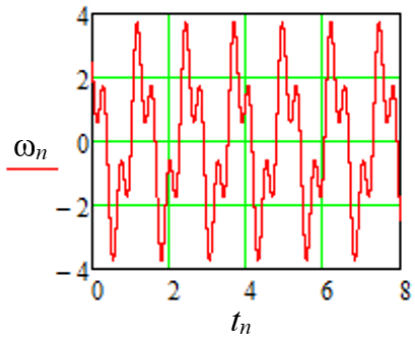

Fig. 3.3. Angular velocity for varying time for tail fin $\lambda_3 = -0.1$.

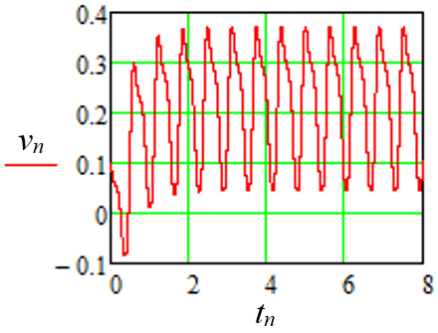

Fig. 3.4. Hull velocity ahead $\lambda_3 = -0.1$.

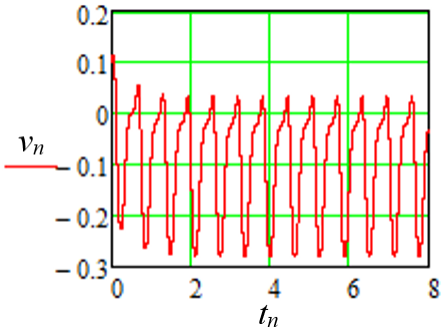

Fig. 3.5. Hull velocity in reverse $\lambda_3 = +0.1$.

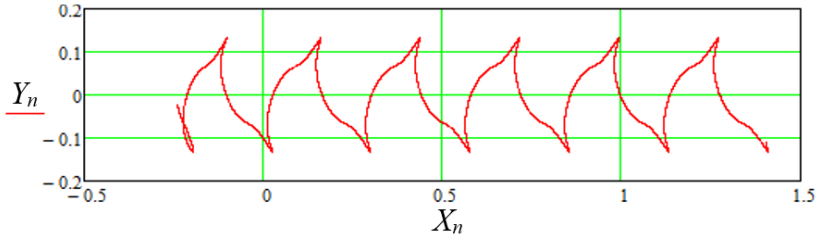

Fig. 3.6. Absolute trajectory of tail point B, moving forward in plane (X, Y), $\lambda_3 = -0.1$.

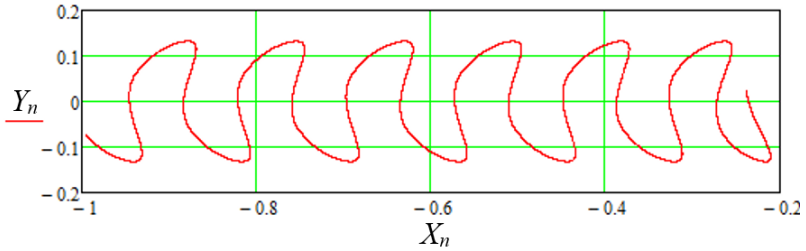

Fig. 3.7. Absolute trajectory of tail edge point B, moving backward in plane (X, Y), λ_3 = +0.1.

3.2. Double Pendulum Motion Analysis in Variable Fluid Flow

This subchapter of Part 3 of the set of scientific publications of the dissertation analyses the motion of double plate oscillations in the vertical plane, interacting with the fluid (air) flow. The model consists of two plates that are interconnected by a rotary hinge and one of them is also connected to the base by a rotary hinge. The case where the fluid flows in a horizontal direction but the plates move around the hinges in a vertical plane is considered (Fig. 3.8 a). An experiment was performed in a wind tunnel (Fig. 3.8 b) at different flow rates, after its analysis an analytical model was created.

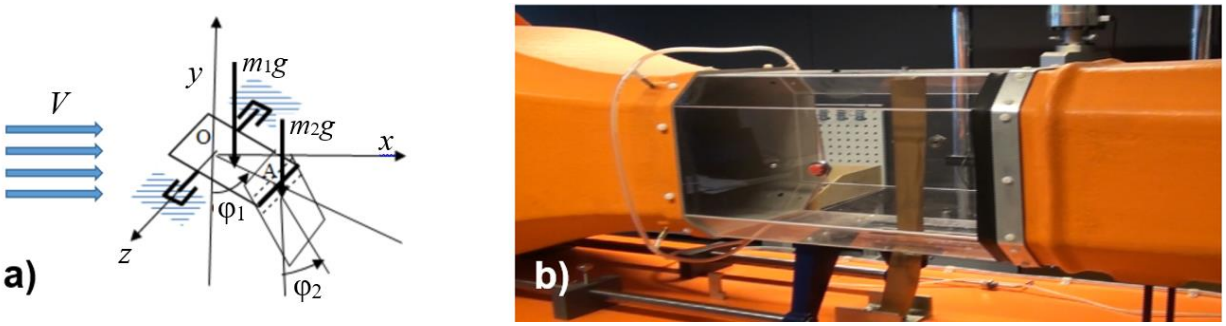

3.8. att. a) dubultplāksnes shematiskais modelis; b) "Armfield" zemskaņas vēja tunelis.

The fluid flow is assumed to be laminar. The interaction of plates with flow is described as the localized interaction of particles with plates, using changes in the centre of degrees of freedom is being studied. The interaction with the liquid is approximated by the quadratic relation to the relative velocity of the flow, taking into account the direction of movement. The obtained system of equations is used for motion simulation (publication No. 18[23]).

As the flow rate increases, the frequency of the plate oscillation cycle increases accordingly (Fig. 3.9). Approximating the second order polynomial at all flow rates the correlation coefficient R_2 is close to 1.

[23] http://tf.llu.lv/conference/proceedings2015/Papers/071_Viba.pdf.

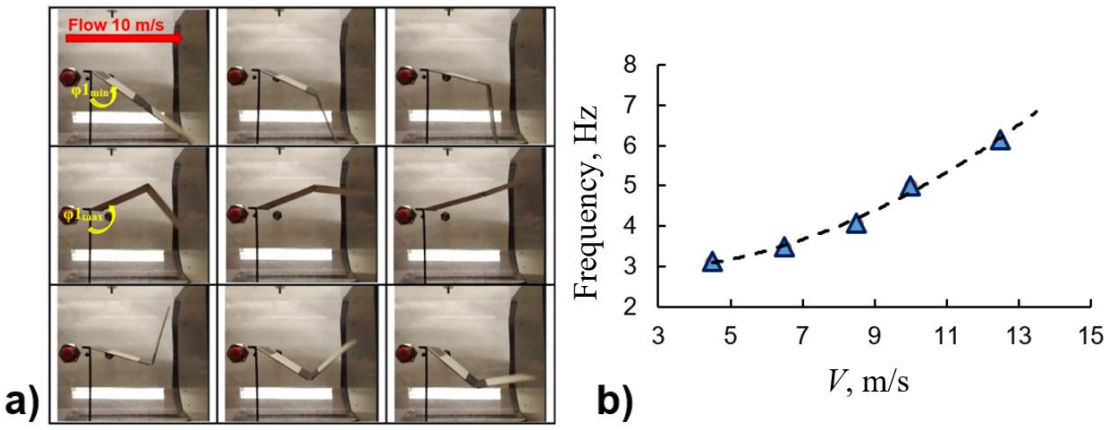

Fig. 3.9. a) The oscillation cycle of the double plate pendulum model at a flow rate of v = 10 m/s[1]; b) frequency of one oscillation cycle depending on the flow rate.

Differential equations of double pendulum motion

To find differential equations of motion for the system with two degrees of freedom, the principle of virtual work[24] was applied. Virtual displacements δr_A δr_{C2} of points A and C2 can be expressed: $\delta r_A = L_1 \delta\varphi_1; \delta r_{C2} = r_2 \delta\varphi_2$, where $\delta\varphi_1, \delta\varphi_2$ – angular virtual displacements of the first and second plates.

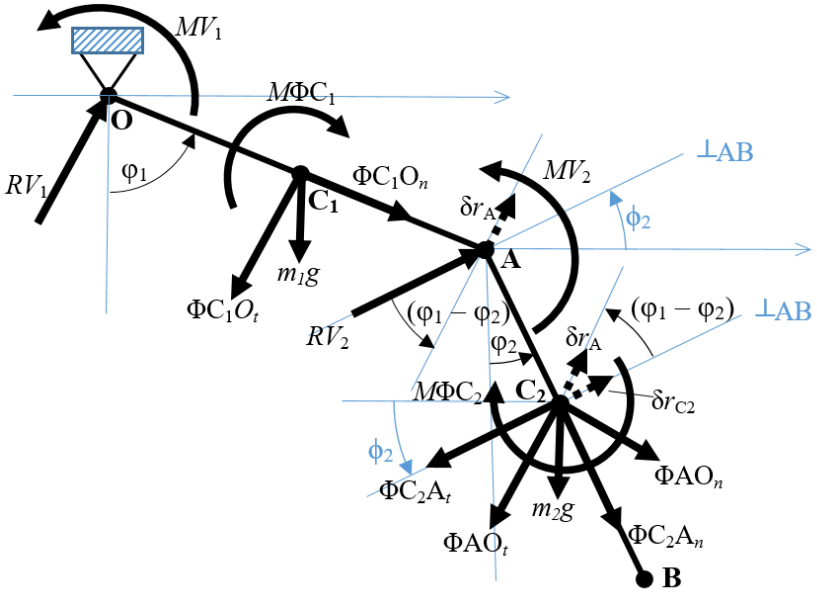

Fig. 3.10. Scheme of forces for principle of virtual work.

[24] Goldstein H., Poole C., Safko J. Classical Mechanics, third edition, Addison-Wesley, 2002, 647 p.

Differential equations of motion for plates:

$$\begin{aligned} &MV_1 - \left(J_1 + m_1 \cdot r_1^2 + m_2 \cdot L_1^2\right)\ddot{\varphi}_1 - m_1 g r_1 \sin\varphi_1 \\ &+RV_2 L_1 \cos(\varphi_1 - \varphi_2) - m_2 r_2 \ddot{\varphi}_2 L_1 \cos(\varphi_1 - \varphi_2) \\ &-m_2 r_2 \dot{\varphi}_2^2 L_1 \sin(\varphi_1 - \varphi_2) - m_2 g L_1 \sin\varphi_1 - MG_1 = 0; \end{aligned} \tag{3.10}$$

$$\begin{aligned} &MV_2 - \left(J_2 + m_2 r_2\right)\ddot{\varphi}_2 - m_2 L_1 \ddot{\varphi}_1 r_2 \cos(\varphi_1 - \varphi_2) \\ &+m_2 \dot{\varphi}_1^2 L_1 r_2 \sin(\varphi_1 - \varphi_2) - m_2 g r_2 \sin\varphi_2 - MG_2 = 0, \end{aligned} \tag{3.11}$$

where RV_1, RV_2 are the main vectors and MV_1, MV_2 are main moments of fluid flow interaction at points O and A; g is free fall acceleration; J_1, J_2 are moments of inertia pendulum parts; $\dot{\varphi}_1, \dot{\varphi}_2, \ddot{\varphi}_1, \ddot{\varphi}_2$ are angular velocities and angular accelerations of pendulum parts with mases m_1 and m_2; MG_1, MG_2 are damping forces moments, e.g., generators interactions.

Graphics of modelling Equations (3.10) and (3.11) in the case of linear interaction forces are shown in Figs 3.10–3.12, with parameters $V_0 = 2$ m/s, $\lambda_1 = 0.2$; $\lambda_2 = 0.4$; $\alpha_2 = 0$, (the flow velocity function V can be expressed in Fourier series members as the function of time t: $V = V_0\left[1 + \lambda \sin(pt) + \lambda_2 \sin(2pt + \alpha_2) + \lambda_3 \sin(3pt + \alpha_3) + \ldots\right]$).

Comments about the motion characteristics are given under the graphics below.

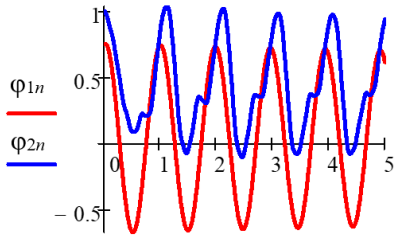

Fig. 3. 10. Graphics of rotation angles for plates. Motion is very stable with low transition process.

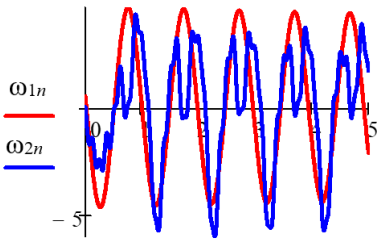

Fig. 3. 11. Graphics of angular velocities.

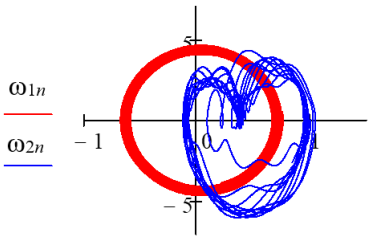

Fig. 3. 11. The phase-plane of plate's motion. After the transition process the motion of the second plate stabilizes.

3.3. Drag Force Reduction for Propulsion System of a Motorized SUP Board Equipped With Waterjet

In the last subchapter of Part 3 of the set of scientific publications of the dissertation, water resistance simulations for the construction of board drive fin water inlet/outlet channel of a motorized SUP (Stand Up Paddle) board were performed (Fig. 3.13).

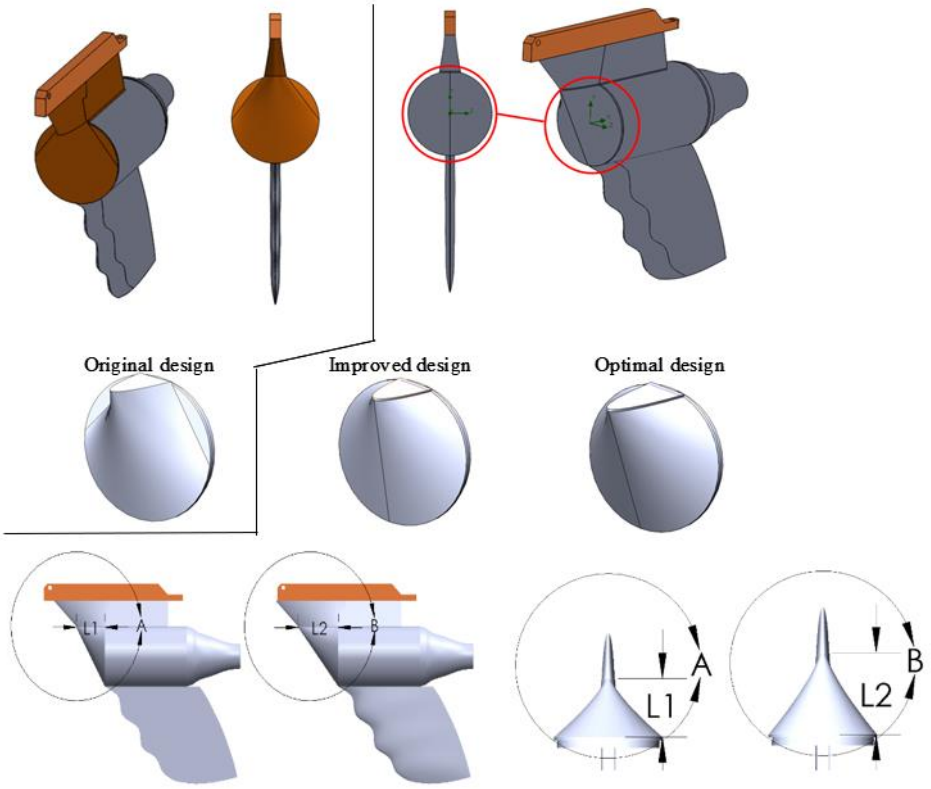

Fig. 3.13. The fin and waterjet view before (on the left side) and after (on the right side) modifications, rounding-off edges and streamlining in SolidWorks.

The drive fin is attached to the board and is fixed with a standard mechanism. The calculation was performed using SolidWorks Flow Simulation software with the aim of improving the shape of the drive fin pressure zone with minimal drag force from the fluid flow and, possibly, a higher inlet velocity ratio. The simulation results showed that the shape of the pressure zone creates significant frontal resistance, the calculations showed that rounding of the edges provided a 35 % reduction in the resistance coefficient, but further refinement reduced it to an additional 10 %, publication No. 23 (under publication process, full paper in the appendix in promotion work).

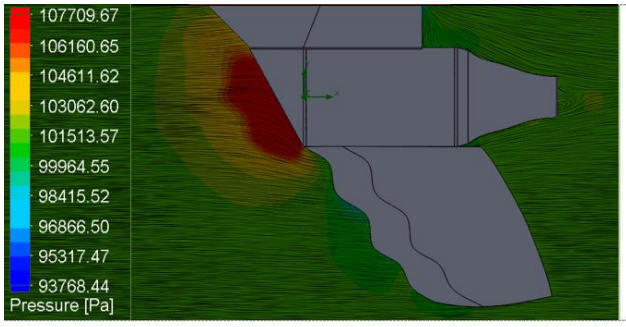

Fig. 3.14. The example of the simulation of the flow around the body. Pressure distribution and streamlines.

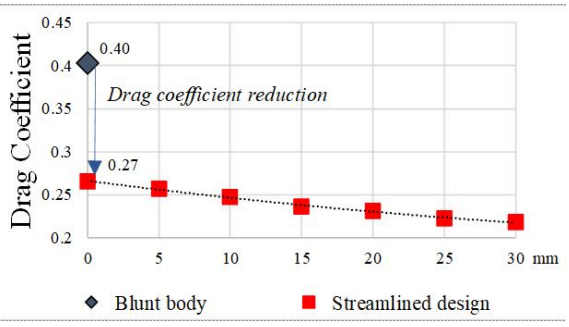

Fig. 3.15. Drag coefficient and reduction after rounding-off the edges of the waterjet duct.

CONCLUSIONS

1. In Chapter 1 of the dissertation, the development of a numerical model for a skeleton with a slider on a sloping plane provides an opportunity to predict movement over a much longer section of the track, taking into account the coefficient of ice friction, aerodynamic resistance, parameters describing the elasticity of the runner and the profile of the surface (the maximum length of Sigulda bobsled push-start facility is 50 m, length of the tracks used in athletes' competitions is on average 1200 m).
2. Using the laws of classical mechanics, it is possible to analytically determine the coefficient of friction of ice and the coefficient of aerodynamic drag. At the input parameters there is a required velocity at certain time or displacement points, at the time sensors, in at least two stages. In skeleton sports and other winter sports, the method can be used if the velocity exceeds 6 m/s and the stages considered are short enough to assume that the Drag coefficients in the stages are constant. The novelty of the method provides an opportunity to simultaneously determine both the coefficient of friction of ice and the coefficient of air resistance, opening wide possibilities for its application in practice.
3. From practical experiments it can be concluded that by increasing the stiffness of the runner of the skeleton sled runners the tension range used by athletes and the frequency of vibrations caused by frictional forces decreases in the direction of movement and practically does not change in the vertical direction. Changes in the stiffness of the runner practically do not affect the natural frequencies of 15 Hz and 71 Hz during the sliding movement. The developed 6 DOF mathematical model for determining the natural frequencies of skeleton sledges allows to easily and quickly determine the approximate natural frequencies, knowing the values of the parameters of the skeleton sledge and runners' stiffness. The experimental results are additionally influenced by the environmental conditions in which the elastic properties of the runner change (not considered in this work additionally).
4. In Chapter 2 of the dissertation a new method has been developed for calculating the approximate flow and still body interaction: for a moving rigid body with a low air flow velocity, for a still body in an air flow, and a moving prism in an air flow. It is assumed that the fluid flow is laminar, the fluid is incompressible, and the viscosity of the fluid is not taken into account in the mathematical modelling, but as an alternative, the interaction factor (constant) is used.
5. A stable result is obtained for energy extraction with variable-area prisms. Although the obtained power is small, the proposed theory (superposition principle) helps to identify the cause and gives an opportunity to work on improving efficiency. The proposed principle explains the mathematical essence in an easy-to-understand and direct way. It was found that an alternative approach to calculating energy production of solid-fluid (air) interaction phenomena using a simple mathematical model is practicable without the use of traditional CFD vortex-induced vibration methods.

6. The method developed in this work helps to perform simple analysis, optimization and synthesis tasks for the interaction of rigid body objects with fluids and with an object in the translational motion taking into account only the body-fluid interaction coefficient. The theory can be applied to the interaction of body-fluid of any complexity if it is intended for mathematical activities.
7. Chapter 3 of the dissertation deals with underwater vehicles where vibrations of stable structures, such as the tail wing or wings, from a constant fluid flow can be caused if the mechatronic control system changes the field of action of the plate. Stationary vibrations occur very quickly, within a few cycles. The instantaneous power of the obtained generator is small due to the area of small perforated plates. Parameter optimization is required to improve efficiency.
8. In order to ensure the continuous operation of underwater robots, it must be possible to switch the mechatronic control system from the movement of the hull diving cycle to the movement of the power filling cycle in the air flow. Energy replenishment is also possible underwater. In this case, an underwater stream must be used. The engineering calculation method proposed in the study allows to analyse the interaction of movements of various objects and liquids. The method allows to model the complex movement of an object in a liquid.
9. In a real fluid flow (air or water), the velocity is not constant but varies over time. This characteristic creates a stable vibration movement in a double pendulum system. The practical results of the experiment in a wind tunnel show that the model has many opportunities for further research: development of an energy production prototype; power measurements for mathematical model validation; generator control optimization at variable flow rates.
10. After 3D flow stimulation, it can be concluded that two types of methods can be used to determine the flow resistance coefficient. In the first, it is focusing only on a local volume area of the viewed object. In the second case, it is looking at the whole object in volume with automatically specified-adaptive finite element size. The difference in results is less than 5 %, therefore it is useful to use the first method to determine the resistance factor reducing the computational time and data storage resources several times and reducing the possibility of misinterpreting the effects of flow turbulence, if not considered separately.